



Proceedings of the Seventh International Conference on
Artificial Intelligence, Soft Computing, Machine Learning and Optimization,
in Civil, Structural and Environmental Engineering
Edited by: P. Iványi, J. Kruis and B.H.V. Topping
Civil-Comp Conferences, Volume 11, Paper 1.1
Civil-Comp Press, Edinburgh, United Kingdom, 2025
ISSN: 2753-3239, doi: 10.4203/ccc.11.1.1

Digital Twin of the Reinforced Concrete Slab Based on the Artificial Neural Network

P. Lacki, A. Derlatka, J. Niemiro-Maźniak and M. Lacki

**Czestochowa University of Technology,
Poland**

Abstract

The article presents a Digital Twin of the reinforced concrete slab to analyse the load-bearing capacity using artificial intelligence algorithms. To achieve this goal, the authors developed three-dimensional parametric numerical model of slab using the finite element method (FEM). When design the numerical model of reinforced concrete members, it is particularly important to select the concrete material model, the type of finite elements of concrete and reinforcing bars, and interactions between these elements. The parametric model served as the base for generating a comprehensive set of solutions, which were subsequently used to train an artificial neural network (ANN). This neural network was designed to predict the behaviour of the slab. By training the ANN with this extensive dataset, the authors of the paper aimed to create an efficient and accurate tool capable of reproducing the structural characteristics of the reinforced concrete slabs. For all analysed variants, boundary conditions were assumed reflecting the slab restrained over the entire perimeter. The numerical analysis was carried out in the ADINA System program.

Keywords: digital twin, artificial neural network, finite element method, reinforced concrete, genetic algorithm, slab.

1 Introduction

Reinforced concrete (RC) slabs are a structural element that transfers loads to beams and columns. Traditional steel bars used as reinforcement of slabs are subject to a natural and inevitable corrosion process, especially in a highly aggressive

environment, which adversely affects the ultimate limit states (ULS) and serviceability (SLS) of the entire structure of concrete slabs [1].

The reaction of reinforced concrete slabs and beams to static and dynamic loads has been studied in recent years not only by experimental tests, but also with using numerical simulations. When design the numerical model of reinforced concrete members, it is particularly important to select the concrete material model, the type of finite elements of A used the Concrete Damage Plasticity (CDP) material model. Cracking under tension and crushing under compression of the concrete are considered the two common failure mechanisms of the CDP model. The reinforcing bars behaviour in the numerical models presented in [2–6] was introduced as elastic–plastic material model.

When selecting the numerical model of reinforced concrete structures, the size of a finite element mesh should also be taken into account. A summary of the mesh sizes that was used in the works [2–10] to simulate reinforced concrete slabs is presented in Table 1. In addition to the dimensions of the finite elements, information on the type of selected elements as well as the edge length ratio was selected. The edge length ratio was defined as the ratio of the concrete finite element length and the slab edge length, where h_f was taken as the edges corresponding to the height of the slab, and l_x was taken as the edges corresponding to the length of the longest edge of the slab.

Particularly noteworthy is work [2], which presents the validation of the numerical model with the results of experimental tests of a two-way reinforced concrete slab subjected to impacting drop weight loading. A continuum 3-D 8-node solid element (C3D8R) was used to discretize concrete part. The reinforcing steel bars was modelled by a 20 mm long 2-node beam elements. The model was validated taking into account the change in the mesh size of the concrete slab, in which a single finite element was equal to 10, 15, 20 and 25 mm. The 10 mm element model with a 16% displacement difference was found to be adequate to predict the slab response in terms of peak displacement under the considered impact load.

The authors of paper [3] presented the results of an experimental evaluation of the use of hemp fibre reinforced polymer (HFRP) fabric sheets as an alternative to carbon fibre reinforced polymer (CFRP) sheets for punching shear strengthening of reinforced concrete slab-column connections. The work [3] also presents the results of numerical calculations carried out using the finite element method with the ABAQUS software. The concrete slab was simulated with 8-node elements of the C3D8R type. The concrete damaged plasticity (CDP) method was adopted for modelling the concrete material. A mesh size of 10 mm was used. The reinforcement was modelled as a 2-node linear 2-D truss element (T3D2) embedded in the concrete element assuming a perfect connection between both materials. A mesh size of 5 mm has been introduced for steel bars. The numerical predictions showed good agreement with the experimental results.

Paper	Software	Concrete slab finite elements	Mesh size of concrete slab, mm	Edge length ratio, %	Reinforcement finite elements	Mesh size of reinforcement, mm
[3]	ABAQUS	8-node, 3D solid elements C3D8R	10	13 for h_f 1.5 for l_x	2-node, linear truss elements (T3D2)	5 mm
[2]	ABAQUS	8-node, 3D solid elements C3D8R	10	13 for h_f 1 for l_x	2-node beam elements	20 mm
[4]	ABAQUS	8-node, 3D solid elements C3D8R	15	25 for h_f 1.6 for l_x	2-node, linear truss elements (T3D2)	15 mm
[5]	ABAQUS	8-node, 3D solid elements C3D8R	20	13 for h_f 0.9 for l_x	2-node, linear truss elements (T3D2)	20 mm
[6]	ABAQUS	8-node, 3D solid elements C3D8R	23	29 for h_f 1.7 for l_x	2-node, linear truss elements (T3D2)	23 mm
[7]	ANSYS	8-node, 3D solid elements SOLID185	$80 \times 80 \times 50$	25 for h_f 4 for l_x	—	—
[8]	ANSYS	3D solid (Solid-65) elements	~50	2.9 for h_f 4 for l_x	linear truss elements (LINK-180)	—
[9]	ADINA System	27-node, 3D solid elements	~187	50 for h_f 5 for l_x	2-node, linear truss elements	~187 mm
[10]	ADINA System	27-node, 3D solid elements	60	30 for h_f 1 for l_x	2-node, linear truss elements	60 mm

Table 1: The summary of the mesh sizes used in the FEM models.

This article analyses the ultimate limit states ULS (stresses in rebars and concrete) and serviceability limit states SLS (cracks and deflections) of single-field concrete slabs, fixed around the perimeter, reinforced with steel bars (Figure 1) assessed by developed Digital Twin based on artificial intelligence algorithms. To achieve this goal, the authors developed three-dimensional parametric numerical model of slab using the finite element method (FEM). The numerical analysis was carried out in the ADINA System program. The parametric model served as the base for generating a comprehensive set of solutions, which were subsequently used to train a neural network. This neural network was designed to predict the behaviour of the slab. By training the neural network with this extensive dataset, the researchers aimed to create an efficient and accurate tool capable of reproducing the structural characteristics of the reinforced concrete slabs.

2 Materials and methods

The subject of the work was slabs with dimensions of 5400×5400 mm, made of concrete class C20/25 with a modulus of elasticity $E_{cm} = 30$ GPa. The material data of the concrete were adopted on the basis of EN 1992-1-1 [11]. Steel rebars (Figure 1) were used for two-way reinforcement of the slabs. The lower reinforcement was placed over the entire surface of the slab and the upper reinforcement was placed around the perimeter in a strip 900 mm wide. Reinforcement material data are presented in table 1.

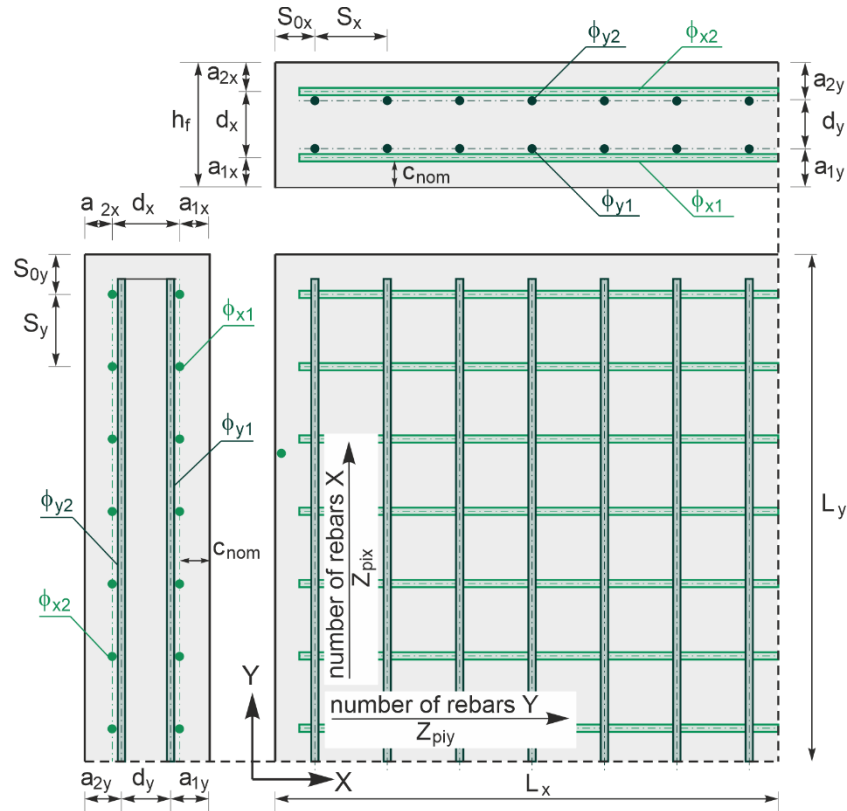


Figure 1: Graph of reinforcement of concrete slabs analysed using numerical models.

Type of rods	Material data		
	Young's modulus E, GPa	Poisson's ratio	Density, kg/m ³
Steel bars	200.00	0.30	7850

Table 1: Properties of applied reinforcing bars.

The thickness of the slab (hf), diameter of lower ($\phi 1$) and upper ($\phi 2$) reinforcement bars and spacing of the rebars ($sy1$) were parameters changed in the numerical model. The combination of parameters given 2160 cases for the developing of artificial neuron network. The parameters were as following:

- thickness of the slab (hf): 100, 150, 200, 250, 300, 350 mm;
- diameter of lower ($\phi 1$) reinforcement: 6, 8, 10, 12, 14, 16, 18, 20, 22 mm;
- diameter of upper ($\phi 2$) reinforcement: 6, 8, 10, 12, 14, 16, 18, 20, 22 mm;
- spacing of the bars ($sy1$): 60, 80, 100, 120, 140, 160, 180, 200 mm.

The analysed slabs were loaded of 10 kN/m² corresponding to a very heavily loaded warehouse floor. The calculations assumed construction class S4 according to EN 1992-1-1 [11] and XC3 exposure class according to EN 206 [12]. The nominal cover for the reinforcing bars in the was assumed to be $c_{nom} = 35$ mm.

The finite element mesh of the slab model with marked boundary conditions is shown in Figure 2.

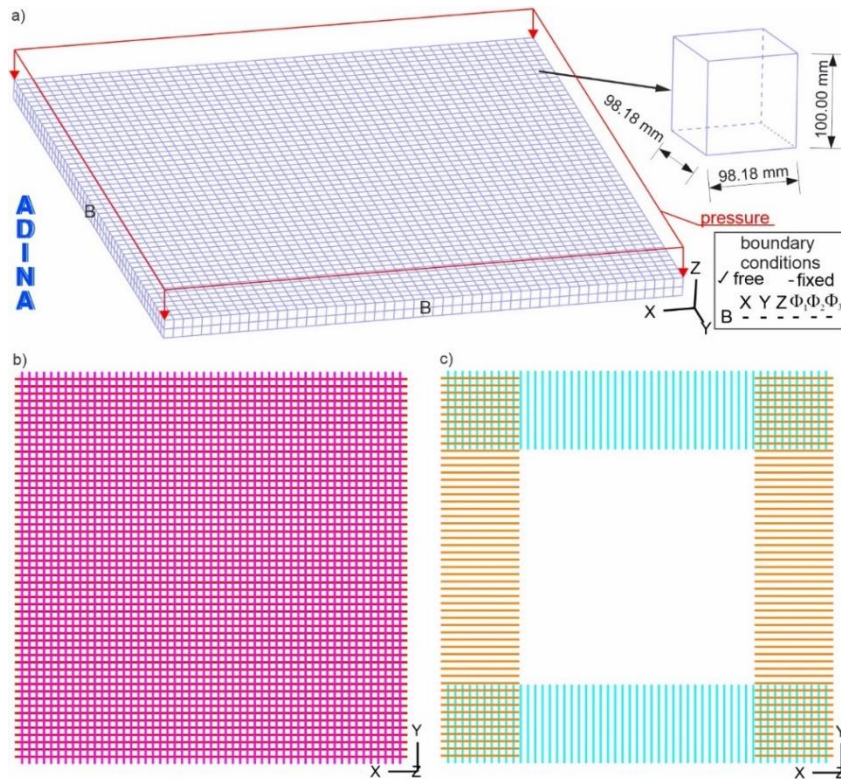


Figure 2: Finite element mesh of concrete slab: a) whole slab, b) lower rebars, c) upper rebars.

In the numerical model, a non-linear analysis was used, taking into account large displacements and large strains. A non-linear model of the concrete material available in the ADINA System program and a plastic-bilinear model of the material of the reinforcing bars were adopted. The concrete slab was modelled using 27-node 3D-solid elements. Rebar elements were used to model the reinforcing bars. In the numerical model of the slab, the finite element method was used to describe the impact of mechanical loads on displacements, type and location of cracks in concrete. Numerical calculations were performed using the ADINA System [13].

3 Results and discussion of parametric FEM model

Based on the numerical analysis, the deflection values of the reinforcement concrete slab from the given loads, were obtained. For each variant, stresses in rebars as well as in concrete component and type and location of cracks were also analysed.

The results of the stresses distribution in rebars of the slab with a thickness of 200 mm reinforced with $\phi = 12$ mm bars were shown in Figure 3 and Figure 4. The maximum value of tensile stress in lower reinforcement is located at the center area of the slab. However, the distribution of tensile stresses in rebars is almost circular. In the lower reinforcement made of SRB bars, compressive stresses (12.16 MPa) reach higher values than tensile stresses (4.28 MPa).

The distribution of stresses in the upper reinforcement made of SRB bars is similar. The reinforcement is predominantly in tension, and the maximum values occur in the middle of the edge in the slab restraint edge. Except that the maximum tensile stress in bars is 16.49 MPa.

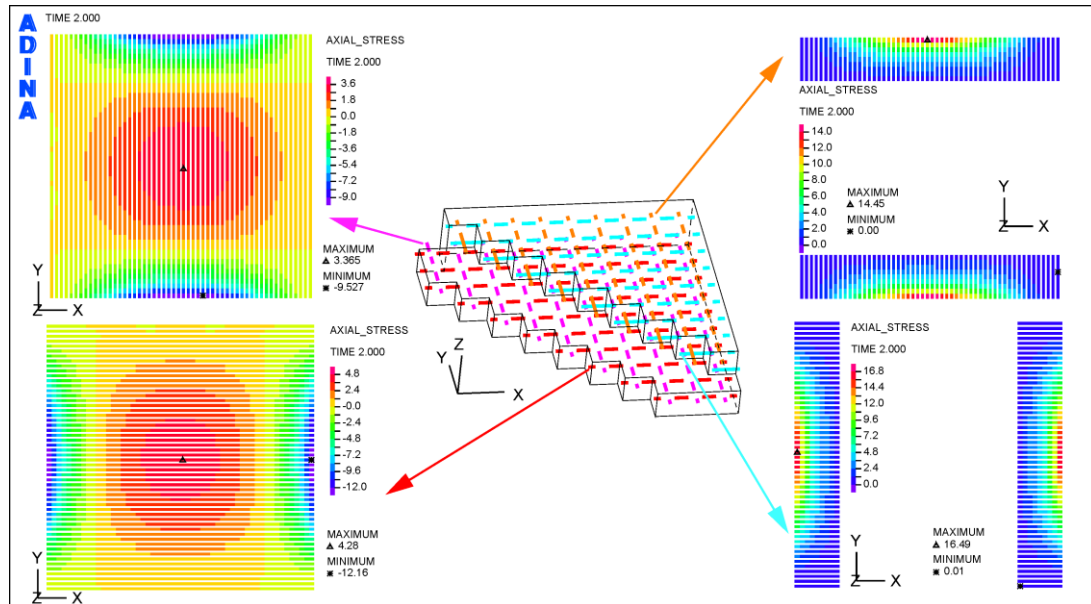


Figure 3: Axial stress in rebars of slab reinforced with $\phi = 12$ mm bars.

The results of the size of displacements and the type of cracks for the concrete slab reinforced with $\phi = 12$ mm bars are shown in Figure 4. Distribution of displacements

indicates that the slab does not sag around the perimeter. What is the effect of slab restraint. The maximum deflections occur in the middle of the slab span. However, on the basis of the distribution of cracks (Figure 4c) it was observed that during the application of a load of 10 kN/m² on the upper surface of the slab, in the area of the middle part of the edge, there are cracks marked no. 1, which corresponds to open cracks. During the application of the load of 100 kN/m² (Figure 4d) on the upper surface of the slab, there are no cracks only in its central part and corners. In the remaining area, open cracks (no. 1), closed cracks (no. 2) and concrete crushing (no. 3) can be observed.

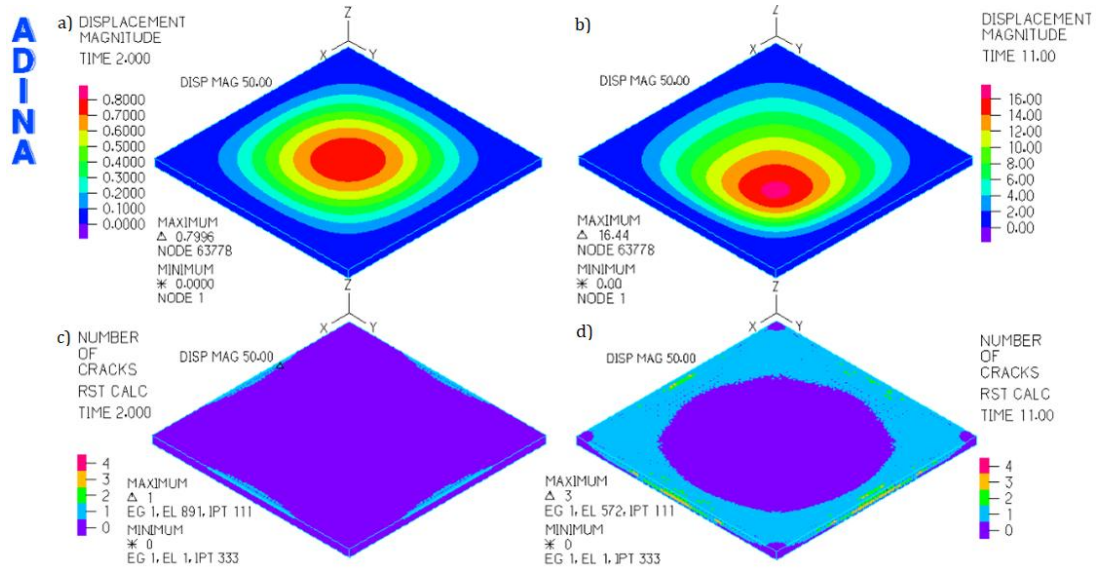


Figure 4: Results of numerical analysis of slab reinforced with $\phi = 12$ mm steel bars: a) displacement distribution at load of 10 kN/m², b) displacement distribution at load of 100 kN/m², c) cracks at load of 10 kN/m², d) cracks at load of 100 kN/m² [14].

3 Artificial neural networks

The samples generated by numerical model were used to develop the artificial neural network. The artificial neural network was constructed for regression. The Multi-Layer Percep-tron (MLP) with the Broyden–Fletcher–Goldfarb–Shanno (BFGS) optimization algorithm was utilized for training. The total of 2160 samples were used to build neural networks. Train-test splitting was used. The samples were divided into three groups: 90% for training the network (learning set), 5% for selecting the network (validation set), and 5% for testing the quality (testing set). The data used for the design of ANN was normalized using the following linear function:

$$y_i = \frac{x_i - x_{min}}{x_{max} - x_{min}} \quad (1)$$

y_i – new value of sample x_i which is scaled,
 x_i – scaled sample,
 x_{min} – minimum value of x set,
 x_{max} – maximum value of x set.

The learning process was monitored by observing changes in error values across different learning epochs. Training was halted before overfitting could occur. The regression network learning process was assessed by observing the change in Sum Square Error (SSE). Adjusting the weights and bias in the input and hidden layers were used as ingredients to reduce the error rate. Sum Square Error was considered:

$$SSE = \sum_{i=1}^N (d_i - y_i)^2 \quad (2)$$

d_i – dependent variable,
 y_i – predicted output.

The random seed was equal to 3. The accuracy of designed ANN was assessed by coefficient of determination R^2 . This value represents the extent to which the variance in the dependent variable can be explained by the independent variables. Structure of designed artificial neural network was presented in Figure 5.

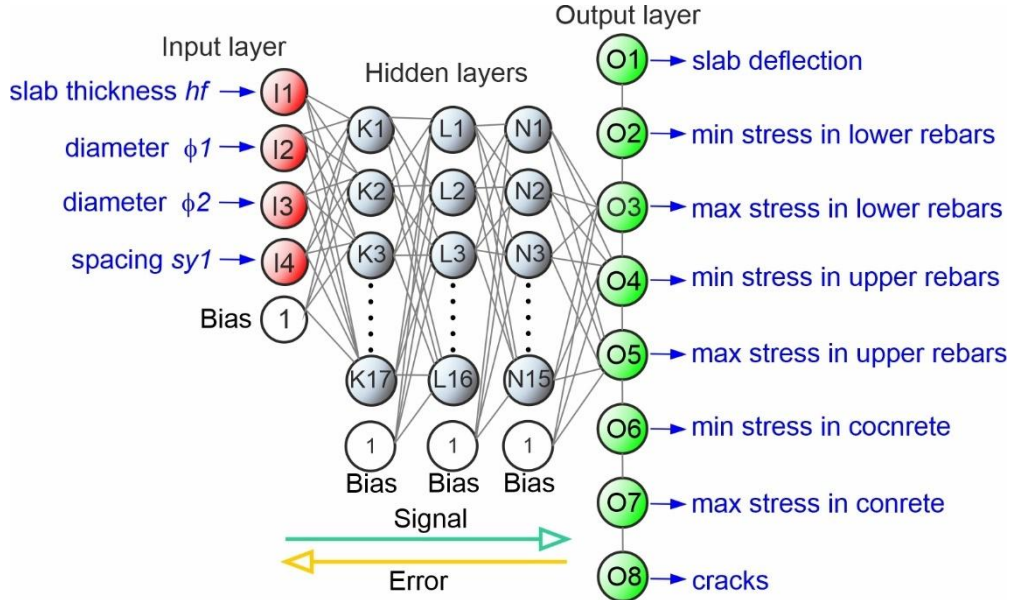


Figure 5: Structure of designed artificial neural network.

Based on the ANN model, the deflection values of the reinforcement concrete slab, the minimum and maximum values of stresses in the lower and upper reinforcement bars as well as the minimum and maximum values of stresses in the concrete slab in its support and mid-span zone as well as the type and location of cracks were analysed.

Traditional optimization and machine learning are both techniques used to solve problems, but they approach problem-solving in different ways. Traditional optimization is used to find the best solution to a well-defined problem with known constraints and objectives. It employs mathematical methods to find optimal solutions. Traditional optimization is generally rigid since the model and constraints are predefined. If the underlying problem changes, the optimization process may need to be adjusted or completely redefined. Depending on the problem, optimization can be computationally expensive but is often more manageable when the problem is

small-scale, well-defined, and mathematically structured. In traditional optimization, once an optimization process is set, it does not adapt unless reconfigured manually. If the system's parameters or environment changes, the model must be updated or resolved.

Machine learning is dedicated to discovering patterns in data. The relationships between variables are not explicitly defined, and solutions lack clear definition. Machine learning adapts through learning from examples, offering greater flexibility compared to traditional optimization methods due to its ability to adjust to new data and learn over time. Techniques such as reinforcement learning enable models to continuously enhance their performance as they acquire more experience or data. However, machine learning can be computationally demanding, particularly when dealing with large datasets or deep learning models. Training ML models may require substantial resources, although this process generally only needs to be performed once or periodically with the introduction of new data. ML models possess the capability to dynamically adapt to new data. For instance, a model can undergo periodic retraining or employ methodologies such as online learning to improve as new data becomes available.

4 Conclusions

- The results of numerical calculations showed the following relationship: the lower the reinforcement coefficient, the greater the deflections of the slabs, which proves that the numerical model of the slab was properly built.
- Crack initiation in concrete occurs under a load of 10 kN/m^2 and can be observed in the form of open cracks located on the even surface of the slab, in the area of the center of the restrained edges.
- Digital Twins can be represented through theoretical models, numerical simulations, as well as artificial neural networks. Developed in this work Digital Twin using ANN algorithms was designed to predict the load carried by RC slabs. The functionality of developed Digital Twin is to predict results for various combinations of parameters without testing them directly. The designed ANN model is able to predict the results of the calculations of RC slab quite accurately based on training data, offering a cost-effective and time-saving alternative to experimental and numerical data collection.

References

- [1] M. Al-Rubaye *et al.*, "Flexural behaviour of concrete slabs reinforced with GFRP bars and hollow composite reinforcing systems", *Compos. Struct.*, 236, 111836, 2020. doi: 10.1016/j.compstruct.2019.111836
- [2] S. M. Anas, M. Alam, M. Shariq, "Damage response of conventionally reinforced two-way spanning concrete slab under eccentric impacting drop weight loading", *Defence Technology*, 19, 12–34, 2023. doi: 10.1016/j.dt.2022.04.011
- [3] L. K. Al-Mawed, B. S. Hamad, "Experimental and Numerical Assessments of Slab-Column Connections Strengthened Using Bonded Hemp Fiber Fabric

- Sheets", *Int J Concr Struct Mater*, 17, 1, 2023. doi: 10.1186/s40069-022-00567-z
- [4] K. Chu, K. M. A. Hossain, M. Lachemi, "Numerical Investigation on Static Behaviour of Steel- and GFRP-Reinforced ECC Link Slabs", *Arab J Sci Eng*, 46, 11, 11027–11045, 2021. doi: 10.1007/s13369-021-05644-1
 - [5] G. J. Milligan, M. A. Polak, "Influence of openings on the punching shear behaviour of concrete slabs supported on special-shaped columns", *Eng. Struct.*, 284, 115968, 2023. doi: 10.1016/j.engstruct.2023.115968
 - [6] E. Yehia, A. Hussein Khalil, E.-E. Mostafa, M. Abdelfattah El-Nazzer, "Experimental and numerical investigation on punching behavior of ultra-high performance concrete flat slabs", *Ain Shams Engineering Journal*, 102208, 2023. doi: 10.1016/j.asej.2023.102208
 - [7] A. Gupta, "Analytical Investigations on Short-Paneled Concrete Pavements Using Finite Element Analysis", *Iran J Sci Technol Trans Civ Eng*, 46, 2, 1755–1770, 2022. doi: 10.1007/s40996-021-00595-x
 - [8] M. A. Adam, A. M. Erfan, F. A. Habib, T. A. El-sayed, "Structural Behavior of High-Strength Concrete Slabs Reinforced with GFRP Bars", *Polymers*, 13, 17, 2021. doi: 10.3390/polym13172997
 - [9] P. Lacki, J. Nawrot, A. Derlatka, J. Winowiecka, "Numerical and experimental tests of steel-concrete composite beam with the connector made of top-hat profile", *Compos. Struct.*, 211, 244–253, 2019. doi: 10.1016/j.compstruct.2018.12.035
 - [10] P. Lacki, A. Derlatka, P. Kasza, S. Gao, "Numerical study of steel–concrete composite beam with composite dowels connectors", *Comput. Struct.*, 255, 106618, 2021. doi: 10.1016/j.compstruc.2021.106618
 - [11] Eurocode 2: Design of concrete structures - Part 1-1: General rules and rules for buildings, EN 1992-1-1, CEN European Committee For Standardization, 2008.
 - [12] Concrete - Specification, performance, production and conformity, EN 206+A2, European Committee For Standardization (CEN), 2021.
 - [13] ADINA System Online Manuals. ADINA R&D, Inc., 2020.
 - [14] P. Lacki, J. Niemiro-Maźniak, "Numerical and Experimental Analysis of Lap Joints Made of Grade 2 Titanium and Grade 5 Titanium Alloy by Resistance Spot Welding", *Materials*, 16, 5, 2023. doi: 10.3390/ma16052038